

## Repair Analysis of Overlay Woven Fabric CFRP Laminates

Osman Çağlar Baysallı<sup>1</sup> , Alihan Cambaz<sup>1</sup> , Yasin Furkan Görgülü<sup>2\*</sup> , Arman Uluoğlu<sup>1</sup> , Umur Ulaş Harman<sup>1</sup> 

<sup>1</sup> Turkish Aerospace Industries Incorporation, Ankara, Türkiye, osmanbysll@hotmail.com, cambazalihan7@gmail.com, armanuluoglu@gmail.com, uuharman@gmail.com

<sup>2</sup> Isparta University of Applied Sciences, Keciborlu Vocational School, Department of Machinery and Metal Technologies, Isparta, Türkiye, yasingorgulu@isparta.edu.tr

\*Corresponding Author

### ARTICLE INFO

### ABSTRACT

#### Keywords:

CFRP Overlay Repair  
Composite Repair  
Prepreg Repair  
Repair Analysis  
Wet Lay-up



#### Article History:

Received: 20.08.2023

Accepted: 09.12.2023

Online Available: 22.04.2024

The increase in aerospace composites usage for structural components demands advanced repair analysis. Overlay repairs of carbon fiber-reinforced polymer laminates offer an alternative that is easier to perform and less time-consuming to produce than the widely used tapered scarf repair and stepped lap. Composite specimen manufacturing was based on both twill carbon/epoxy prepreg and wet lay-up. The repair was performed with both prepreg and wet extra plies to the parent prepreg structure. However, the design of overlay joints must be carefully investigated to avoid generating stress concentration regions at free edges. This study examined specific extra ply terminations' impact on peak stresses in the adhesive bond line. Linear finite element analysis was performed to conduct a maximum principal stress study with a focus on three joint design parameters: ply material, overply effect, and stacking sequence. FEA accurately predicted experimentally observed responses and provided further insight into the failure behavior of the structure. Results showed that overlay joints have a strong sensitivity to ply material type, the number of overply, and stacking sequence. The introduction of overplies provided protection and stiffness at joint tips, and an overply material behavior was identified. The location of  $\sigma$  plies in the composite laminates was highlighted as an important factor. The analysis was then extended to three-dimensional FE models for verification. In conclusion, results showed that high-stress concentration in overlay joints can be mitigated with the introduction of overplies and appropriate changes in joint design parameters to reduce stress peaks at joint tips and corners.

## 1. Introduction

With advancements in technology, the aviation industry has witnessed a significant increase in the use of composite materials. These materials offer exceptional strength-to-weight ratios and corrosion resistance, making them ideal for aerospace applications. The demand for lightweight aircraft structures has driven the adoption of composites in various components, including fuselages, wings, and interior parts. The progress in fiber-reinforced polymer composite materials has led to notable

improvements in the construction of lightweight structures [1].

In recent times, there has been a growing utilization of CFRP (Carbon Fiber-Reinforced Polymer) in airframes and engine components to decrease aircraft fuel usage. CFRP, possessing a minimum yield strength of 550 MPa, exhibits a density that is one-fifth that of steel and three-fifths that of aluminum-based alloys [2]. Despite considerable advancements in aerospace materials, certain obstacles remain, notably the insufficient strength to meet the rising need for lightweight materials [3].

While composites offer numerous benefits, composite structures are prone to various defects that can occur during manufacturing or while in use. These defects have the potential to impact the overall structural integrity, leading to a significant decrease in the strength and stiffness of the composite structure [4–7]. The repair of composite materials plays a crucial role in maintaining structural integrity, ensuring operational safety, and extending the service life of aircraft. However, repairing composites poses unique challenges due to their complex structures, anisotropic behavior, and the need to maintain material performance.

There is a study that evaluates the mechanical performance of damaged steel pipelines repaired with CFRP composites using finite element analysis. Two repair strategies, wrap and patch repair, are analyzed under Maximum Allowable Operating Pressure (MAOP) conditions. Findings suggest that thicker CFRP reduces stress in both the pipe wall and CFRP, and enhancing CFRP reinforcement can be achieved with higher elastic modulus infill materials [8].

Another aim of this research is to perform Finite Element Analysis (FEA) validation of mechanically tested and overlay-repaired aviation composites. The study focuses on evaluating the effectiveness and reliability of overlay repair techniques through numerical simulations. The key goals include assessing the structural performance, load-carrying capacity, and long-term durability of the repaired composite components.

FEA is an important tool in providing consistent data in the analysis and design of composite structures [9]. It enables engineers to simulate and predict the mechanical behavior of repaired composites, aiding in the optimization of repair processes and enhancing repair reliability.

This study also aims to provide a comprehensive analysis of the repair techniques for overlay woven fabric CFRP laminates. It will review the existing literature, highlighting the key findings and advancements in this field. Furthermore, it will present experimental results from the research, focusing on the evaluation of different

repair approaches and their impact on the laminates' performance.

This analysis is intended to contribute to the ongoing efforts to enhance the repair capabilities of overlay woven fabric CFRP laminates and provide insights for the design and implementation of more reliable and efficient repair methods.

## 2. Experimental Work

The manufacturing and repair process of composite laminates was carried out by standard repair procedures for the manufacture and repair of aircraft composite laminates. Made of M21/AS4C/ 40RC/T2/285/6K  $2 \times 2$  twill carbon/epoxy fabric with cure coat thickness 0.285 mm 45/0/45/0/45/0/45 orientations 20 composite samples of 250x25x2 mm dimensions were produced at 180° and 7 bar pressure for 9 hours according to the specifications provided by the manufacturer [10].

The size and geometry of the test specimens were prepared according to the requirements of the ASTM Tensile Test Standard for Polymer Matrix Composites (D3039/3039 M) [11]. 20 mm x 20mm x 1.7 mm laminated part from the center of each sample was removed with 120° or finer sandpaper. The last ply of the sample was left and Hysol EA 9396 resin was injected into it. After the resin injection process was completed, HYSOL 9396 was cured at 66 +/- 2 degrees for 1 hour. Curing procedures were performed per the resin manufacturer's instructions.

After the curing process, 4 different sample types were created with different numbers of extra plies and wet with 12,5 mm overlapping, prepreg methods on the bag side and tool side. The first sample type was cured with 2 extra bag sides and 1 extra from the tool sides with the carbon prepreg method at 180 +/-5 degrees according to the autoclave manufacturer's requirements.

In the second sample type, additional carbons were laid by 2 bag sides and 2 tool sides by prepreg-applied and cured in an autoclave. The third sample type was created by laying extra carbons by the wet lay-up method by 2 bag sides and 1 tool side. The fourth sample type was

created by laying extra ply by 2 bag sides and 2 tool sides. The samples produced with the third and fourth type wet method were cured with HEATCON (heat blanket) in a 650 mmHg vacuum. For the wet method, Hexforce G0904 D 1070 TCT plain weave dry carbon fabric was laid using Hysol EA 9396 resin [10].

The properties of the carbon and resin laid with the wet method are given in Tables 1 and 2 [12]. All extra plies are laid at 45 degrees, and plies with the same orientation as the top ply have been selected. In the first and second sample types, the extra plies were laid with 12,5 mm overlapping using FM-300K film adhesive. FM-300K material properties are given in the table and cured according to the manufacturer's requirements.

After the repair and curing cycle of the prepared samples, they were examined with the help of Manual Ultrasonic Pulse Echo Inspection (MUPE), and defects such as delamination and debond were evaluated. In addition, the porosity values in the samples were observed by the MATEC ultrasonic tester (MA, USA) using the Automatic Ultrasonic Transition Method (AUTT).

Keeping the Porosity values at a 6 dB attenuation difference ( $\Delta$ dB) allows the samples to be accepted for testing. While 6 dB attenuation difference values were observed in the laminated non-resinous regions of the samples, a 15-20 dB attenuation difference was observed in the resin-filled region due to the nature of the resin.

Since the main purpose of the Nondestructive Inspection application is to see the porosity and defects in the laminate, the porosity value observed in the resin does not interfere with the test.

After the samples were inspected, plain tension tests of the samples were carried out according to ASTM 3039 with the Instron 8852 Tensile Testing Machine (MA, USA). The test setup can be seen in Figure 1. a clip-on extensometer was used to get more accurate results in stress and strain measurements.

**Table 1.** Mechanical properties of Hexforce G0904 plain weave dry carbon fabric impregnated with Hysol EA 9396 adhesive, with a 1/3 weight ratio and M21 / AS4C impregnated material [10, 13–15].

Property	Symbol	Hexforce G0904	M21 / AS4C
Elastic Modulus (GPa)	$E_{11}$	49.6	61.0
	$E_{22}$	49.6	61.0
	$E_{33}$	8.0	8.9
Shear Modulus (GPa)	$G_{12}$	3.3	4.2
	$G_{13}, G_{23}$	2.8	3.8
Tensile Strength (MPa)	$X_t$	517	930
	$Y_t$	517	940
Shear Strength (MPa)	$S_{12}$	60	96
	$S_{13}, S_{23}$	34	64
Poisson's Ratio	$\nu_{12}$	0.045	0.05
	$\nu_{13}, \nu_{23}$	0.28	0.3

**Table 2.** Mechanical Properties of the adhesives [13, 15–18].

Property	Symbol	FM-300K	HYSOL EA 996
Tensile Modulus (GPa)	E	3.12	2.7
Shear Modulus (GPa)	G	0.9	0.7
Tensile Strength (MPa)	$t_n^0$	72	55
Shear Strength (MPa)	$t_s^0, t_t^0$	42	26
Tensile Stiffness ( $N/mm^3$ )	$K_n$	15,600	$10^6$
Shear Stiffness ( $N/mm^3$ )	$K_s, K_t$	4500	$10^6$
Toughness in Tension (N/mm)	$G_{IC}$	1.1	0.3
Toughness in Shear (N/mm)	$G_{IIC}, G_{IIIC}$	4.8	0.5

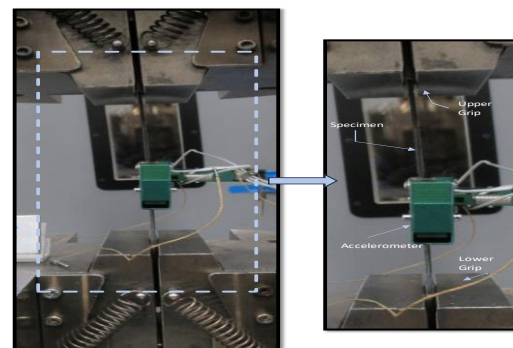


**Figure 1.** Test configuration.

### 3. Finite Element Model and Analysis

A three-dimensional finite element method for the overlay repairs was performed in ANSYS 2021 R1.

Fig 2 presents a schematic two-dimensional view of the model and its boundary conditions including the force of direction and fixed point (fixed joint). Specified material properties, geometry, and dimensions of the 3D model consisting of seven-layered composite laminates bonded by Hysol EA 9396 adhesive are kept the same as in experimental work. Individual plies with  $[45/0/45/0]_s$  pattern were discretely modeled. ply-by-ply surface contact is applied with a multipoint constraint (MPC) algorithm to obtain a perfect bonding between interfaces [19].

Discretized layers meshed with hexahedral 8-node elements were used. Four model fibers are aligned parallel to the loading direction along the x-axis, with overply lap length set at 0.5 inches  $[-45/+45]$  stacking sequence. The 3D finite element model consists of about 750,000 elements, the total number of elements is higher than about 550,000 elements done by Hamza and others [12]. Repair types are different from Hamza's work but the total area of geometry and discretized layers are very consistent with the model.



**Figure 2.** Schematic views of the repair configurations.

Linear static analysis was performed to investigate local peak stress. Primary stress includes peel stress, shear stress, and max principal stress to verify analysis with the help of test results. Peel (Normal) stress is considered along the Z-axis and shear stress was taken for both XY and XZ, but XY shear stress values are neglected as their values are smaller.

Failure load values of four specimens were investigated considering peak stress as given load from the test result. The gathered test results

agree with the observation made in the 3D finite element model. The addition of extra plies and different overply materials provided added stiffness and protection from local stress at adhesive tips.

#### 3.1. Maximum stress theory

Maximum Stress Theory states that failure happens if any stress along the material loading direction exceeds the allowable strength of the material. Five independent strength constants are important for a single ply [17, 20, , 21–28, 29–34]:

- $S_{Lc}$  – Longitudinal Compressive Strength
- $S_{Lt}$  – Longitudinal Tension Strength
- $S_{Tc}$  – Transverse Compressive Strength
- $S_{Tt}$  – Transverse Tension Strength
- $S_S$  – In-plane Shear Strength

To avoid failure, stress values along the loading direction have to be:

$$\begin{aligned} -S_{Lc} < \sigma_{11} < S_{Lt} \\ -S_{Tc} < \sigma_{22} < S_{Tt} \\ -S_S < T_{12} < S_S \end{aligned} \tag{1}$$

If it is the case that the material is loaded with simple tension which means  $\sigma_{xx}$  is present while,  $\sigma_{yy}$  and  $\sigma_{xy}$  values are negligible; three failure scenarios can be taken into account as follows:

1. Longitudinal to fiber direction, failure is primarily caused by fiber fracture:

$$\sigma_{xx} = \frac{S_{Lt}}{\cos^2 \theta} \tag{2}$$

2. Transverse to the fiber direction, failure is primarily caused by matrix or fiber-matrix composition:

$$\sigma_{xx} = \frac{S_{Tt}}{\sin^2 \theta} \tag{3}$$

3. Shear forces cause failure by matrix or fiber-matrix interface, or both at the same time:

$$\sigma_{xx} = \frac{S_S}{\sin \theta \cos \theta} \tag{4}$$

This theory falls short when one would like to interpret the interaction of stresses through all directions and their corresponding mixed failure modes, but it ensures a solid ground if the material is loaded with simple tension.

#### 4. Modeling Results and Discussion

The stress distributions of the four models are initially simulated and presented. Fig 3 demonstrates a comparison of experimental and numerical displacement curves for each overlay model. The results show that the finite element model can closely predict the actual load–displacement behavior.

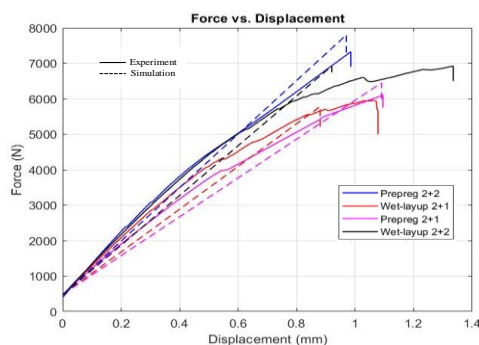


**Figure 3.** Comparison of experimental and numerical load-displacement curves for specimens with the wet lay-up and impregnated extra plies.

An adjustment to the excess of the experimental displacements may result from the positioning of the extensometer in the center of the sample and the subsequent integration of the displacement data. While scarf and step-lap repairs do not exhibit this change, overlapping fixes do [35]. Different stiffness leads to local peak stress variations through the thickness. Fig 4 depicts the 3D finite element peak shear and peel stress in the stress field in four models.

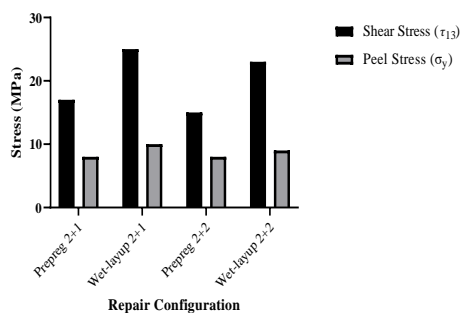


**Figure 4.** Failure peel and shear stress values for all models predicted by simulations.

For the four models, the main differences between wet-layup and prepreg repair stiffness consist of local peak stress along thickness and width which are highest near the free edges of the adhesive-filled area. Average stresses along with approximately constant but we focused on local peak stresses as local peak stresses reach allowable stress limits contributing to failure before average stresses. The stress variation of the four repair models is shown in Fig 4.

The finite element model provides investigation with stress concentration regions. High-stress concentration was observed at the corners contacting the adhesive in all 4 models. High peel and shear stresses were observed in 4 models since the 3-12° taper angle was not observed as in classical scarf repairs. Failure mode changed from cohesive to adhesive failure as the adhesive surface area was greatly reduced.

The adhesive zone creates a load path between the [45/0/45/0]<sub>s</sub> parent structure. Since the adhesive cannot carry a sufficient load due to its low hardness value, shear, and peel stress peaks at the adhesive ends.

Thanks to the nature of the Continuum mechanic approach, stress-strain values are compared with allowable values which are obtained from test results. The singularity values observed in the adhesive-filled corners were eliminated by fine meshing. The absence of a progressive bonding surface such as step-wise or taper between the parent structure and the adhesive causes adhesive failure. Adhesive failure resistance values are much lower than cohesive failure, so it is not a desired failure.

##### 4.1. Maximum stress theory

Since Hysol EA9396 resin is a brittle material, it was also modeled above the thickness limits preferred in aviation, so the extra plies directly affected the strength. The maximum stress values observed at the points where the plies were in contact with the adhesive caused the failure.

The crack that started in the adhesive corners advanced in the 45° direction and exceeded the maximum shear strength of Hysol ea 9396. Since the overlap distances of the extra-laid carbons

were to be fixed above a certain limit, overplies of 12.5 mm were set. Extra-laid prepreg carbon plies were adhered using FM-300K film adhesive, causing potential porosity areas. Lower dB losses were observed in the carbons laid by hand layup in clean room conditions, compared to the models applied with the prepreg method.

Since the defects in the material directly affect its characterization, the differences in strength values in the models with extra laying vary between 15-20%. Since the stiffness values of the prepreg models are higher than the wet method, higher strength values were observed compared to the wet method.

#### 4.1. Effect of overply

Since the lap length is set to 12.5 mm, the main purpose of this article is to investigate the lacquer peak stresses that cause failure. In prepreg models, the effect of one extra individual 1 per 45° layer is about 15% power. The effect of the extra 45° layer is around 15% in the models laid with the wet method.

Peak stress fields observed at the tip of the adhesive cause the adhesive to deteriorate. Peel stress values are symmetrical along the x-axis from the center of the adhesive-filled area.

While shear stress values were found to be maximum at the adhesive ends, higher stress values were observed compared to the shear stress values. Shear stress values reach a maximum along the x-axis from the area filled with the adhesive to the ends.

The reason for limiting the number of extra plies in the building to 3-4 ply is to eliminate factors such as the human factor during the preparation of the prepreg model that will affect the behavior of the material, such as the porosity effect.

Since the symmetry is broken in the overlay models due to extra ply, bending occurred in the model, and local compressive stresses were observed. In the unsymmetrical extra plies, the highest stress values were obtained by making a finer mesh on the load path. These results are in good agreement with the test results.

## 5. Results and Discussion

M21 / AS4C composite material is produced in 4 models as its main structure. While an extra layer was laid on the area filled with the adhesive in the parent structure with the prepreg method, FM-300K was used while the extra layer was laid with the wet laying method, while Hysol EA9396 was used. Models laid with M21 / AS4C laminate showed higher strength thanks to its stiffness. However, the potential for porosity in the extra layers laid with FM-300k changes the failure mode. In this study, it was observed that the extra plies laid with the prepreg method caused the cohesive failure.

As can be seen in Figure 5, the extra-laid carbons did not cause undesired adhesive failure with good adhesion.

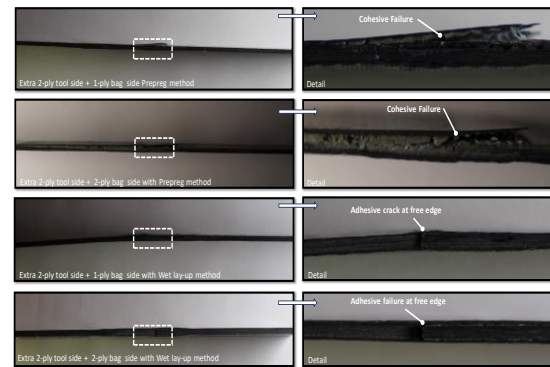


Figure 5. Failure cross-section of four models.

However, the failure loads in the Wet-layup method are satisfactory compared to the Prepreg method. Although wet lay-up repair stiffness values are low, HYSOL EA 9396 bonded adhered well to the adhesive-filled area.

Because lower  $\Delta$ dB were observed in the wet lay-up method, it prevented the expected failure load differences between repair models produced by the prepreg and the wet lay-up.

While 90-degree cracks were investigated in the adhesive-filled area in the samples with extra laying with the wet method, 45-degree cracks were observed in the adhesive-filled area in the samples that were extra-laid with the prepreg method.

The additional prepreg carbon-laid samples had higher local peak stresses, which sped up fracture

propagation. The load inputs and failure loads of the test samples from the extensometer were examined in the analyses. The extensometer adhesive was above the filled zone, which led to oscillation in the curve, which resulted in bearing damage and fractures.

While the adhesive was filled in the middle of the unrepaired samples, sandpaper caused buckling at the ply ends and the discontinuity in the structure caused heavy bearing damage at the edges of the adhesive-filled region.

It is produced as the parent structure of M21 / AS4C composite material in 4 models. FM-300K was used when laying extra ply on the shadow filled with the adhesive in the main structure with the prepreg method, and Hysol EA9396 was used when laying the extra ply with the wet lay-up method. Models laid with M21 / AS4C laminated showed higher strength due to its rigidity.

However, the porosity potential in the extra lays laid with FM-300k changes the failure mode. In this study, it was observed that the extra plies laid with the prepreg method caused the cohesive failure.

As can be seen in Figure 5, the extra-laid carbons did not cause undesired adhesive failure with good adhesion.

CFRP laminate specimens are modeled ply-by-ply and discretized because the composite structure is not homogeneous and is anisotropic. Lamina or ply analysis addressed and determined properties of plies which are oriented at an angle to the loading axis. Composite laminates are normally thin compared to their length and width and are loaded in plane stress conditions. This paper emphasized in-plane loading.

As shown in Fig 4., for positive shear stress, the maximum tensile stress is parallel to the fiber direction and is supported by strong fibers, if shear stress is negative, maximum tensile stress is perpendicular to the fiber direction and the matrix supports the load. Thus, a positive shear stress leads to higher load-carrying capability than a negative shear stress. Elastic constants of both on-axis and off-axis plies are obtained and used to predict overall laminate response using

maximum stress theory. Laminate theory estimates laminate behavior fairly accurately in the interior of the laminate.

However, within about one laminate thickness of free edges, lamination theory breaks down and fails to predict large interlaminar stresses that can develop. Large interlaminar stresses developed leading to bearing damage and adhesive cracking at the edges. Edge effects arise as a result of the requirement for strain compatibility between plies in laminate and adhesive-filled areas. Interlaminar shear and through-the-thickness peel stress develop near the free edges of laminate contact with the adhesive-filled area.

The principal reason for the development of these interlaminar stresses is a mismatch of Poisson's Ratio ( $\nu_{xy}$ ) and coefficients of mutual influence between adjacent plies. The difference in Poisson's ratios leads to different transverse contractions. This leads to interlaminar shear stresses between plies and the Hysol EA 9396 filled area. The adhesive-filled area created a free edge that led to the discontinuous middle of specimens. Interlaminar shear stresses between plies, forcing zero-degree ply to expand in the transverse direction and the 45-degree ply to contract.

The shear force is confined to the edge because once the required tension ( $\sigma_{yy}$ ) is established in zero-degree ply, compatibility is ensured across the middle of the laminate part. Shear stress obtained maximum at free edges,  $\sigma_{yy}$  a turning moment is produced thus to balance this moment, peel stresses develop in laminate with distribution indicated in figure 6. The strain observed in the specimens is shown in Figure 7. The tensile test results of the experiments obtained according to different layouts are given in table 3.

**Table 3.** Summary of the tensile testing results.

Specimen Type	# of Specimens Tested	Average Tensile Strength	Max Tensile Strength	CoV (%)	Recovery Rate
Extra Wet laid 2+1	5	119	128	7.0	22.8
Extra Wet laid 2+2	5	146	150	2.6	28.1
Extra Prepreg laid 2+1	5	132	141	6.3	25.3
Extra Prepreg laid 2+2	5	154	164	6.0	29.6
Intact	5	520	560	7.1	-

In the analysis of the 2+1 sample of the Extra Prepreg, it is observed that the top ply, having a higher stiffness than the resin, bears the load, leading to the initiation of delamination from the top ply. As only a single extra ply laid on the bag side is incapable of transferring the load, it separates and subsequently transfers the load to the resin, resulting in cracking at the free edge of the resin. As indicated in the analyses, maximum stress and strain values are observed in the free edge regions.

In the examination of stress and strain values in the 2+2 sample of Extra Prepreg, it exhibited a behavior similar to the 2+1 sample of Extra Prepreg, but due to the additional 1 ply effect, it failed at higher stress and strain levels. As illustrated in Figure 5, ply delamination was followed by film adhesive separation. The film adhesive separation causing cohesive failure continued along the resin free edges. Stress and strain values causing cohesive failure are observed in the resin free edges.

Upon examining the failure of the Extra Wet laid 2+1 sample, the reason for its differing appearance from the Extra Prepreg Laid 2+1 and Extra Prepreg Laid 2+2 samples lies in the inherent nature of the wet method, which does not necessitate the use of film adhesive. Similar to prepreg methods, the region filled with resin after the top ply delamination in the wet method failed as it could not transfer shear flow.

The wet approach's credibility for on-site repairs is increased when it exhibits behavior similar to the prepreg method. As evident in the analysis results, there is an approximate reasonable difference of about 3%.

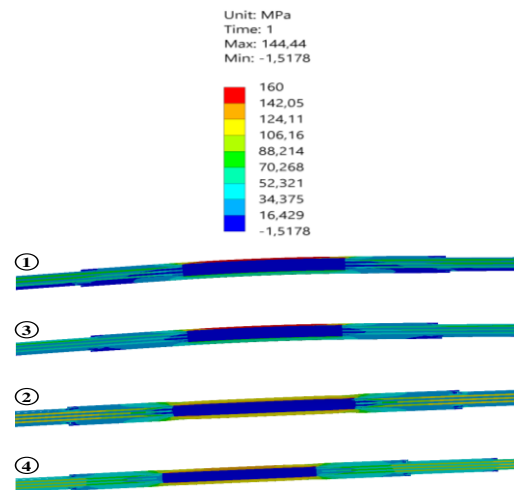


**Figure 6.** Stress results of CFRP laminate repaired: (1) extra wet laid 2+1, (2) extra wet laid 2+2, (3) extra prepreg laid 2+1, (4) extra prepreg laid 2+2.

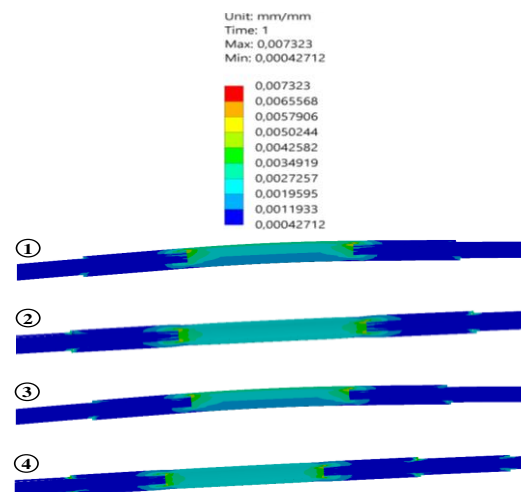


**Figure 7.** Strain results of CFRP laminate repaired: (1) extra wet laid 2+1, (2) extra wet laid 2+2, (3) extra prepreg laid 2+1, (4) extra prepreg laid 2+2.

In both the Extra Wet Lay-up 2+2 and Extra Prepreg Lay-up 2+2 samples, a symmetrical condition was achieved by adding two extra plies, resulting in both analysis and test outcomes showing no bending and being subjected to pure tension loading. In repairs using wet methods, the absence of film adhesive led to higher shear stress values, causing the structure to fail. As observed in the analysis results, failures were evident at 0.7% tension strain values.

When compared to the manufacturer-supplied strain value of 1.62% tension strain in the intact laminate structure, it was observed that separation occurred from the region in contact with the resin due to shear effects, without adherent failure.

## 6. Conclusion

In this study, both the number of extra plies and the repair technique (prepreg or wet lay-up) significantly influence the durability of the overlay + resin potted repair have been demonstrated. From the experimental findings, it is evident that as the number of additional plies approaches the thickness of the initial laminate stack-up, the strength of the repair increases. Specifically, prepreg repair techniques exhibited marginally higher tensile strength compared to wet lay-up overlay repair.

Comparatively, the FEA corroborated these experimental results, illustrating a similar trend in strength enhancement with increased ply numbers and favoring the prepreg method. The FEA also provided deeper insights into the stress distribution and potential failure points, which were observed to align with the experimental outcomes. Notably, cohesive failure was predominantly observed in prepreg repairs, a finding that was mirrored in the FEA through stress concentration analyses. Conversely, adhesive failures near the free edges of the resin-potted region, primarily seen in wet lay overlay repairs experimentally, were also predicted by the FEA models.

The congruence between the FEA and experimental results strengthens the validity of our findings. Further investigations, as highlighted by both methodologies, will focus on exploring the effects of varying overlap amounts and the impact of symmetric laminates with greater thickness than the tested laminate. This future research aims to refine our understanding of the repair mechanics and optimize repair methodologies for enhanced durability.

### Article Information Form

#### *Funding*

The authors have not received any financial support for the research, authorship or publication of this study.

#### *Authors' Contribution*

The authors contributed equally to the study.

#### *The Declaration of Conflict of Interest/ Common Interest*

No conflict of interest or common interest has been declared by the authors.

#### *The Declaration of Ethics Committee Approval*

This study does not require ethics committee permission or any special permission.

#### *The Declaration of Research and Publication Ethics*

The authors of the paper declare that they comply with the scientific, ethical and quotation rules of SAUJS in all processes of the paper and that they do not make any falsification on the data collected. In addition, they declare that Sakarya University Journal of Science and its editorial board have no responsibility for any ethical violations that may be encountered, and that this study has not been evaluated in any academic publication environment other than Sakarya University Journal of Science.

#### *Copyright Statement*

Authors own the copyright of their work published in the journal and their work is published under the CC BY-NC 4.0 license.

### References

- [1] P. Balakrishnan, M. J. John, L. Pothan, M. S. Sreekala, S. Thomas, "Natural Fibre Composites and their Applications in Aerospace Engineering," 2014.
- [2] D. K. Rajak, D. D. Pagar, P. L. Menezes, E. Linul, "Fiber-reinforced polymer composites: Manufacturing, properties, and applications," *Polymers*, vol. 11, no. 10, 2019.
- [3] B. Parveez, M. I. Kittur, I. A. Badruddin, S. Kamangar, M. Hussien, M. A. Umarfarooq, "Scientific Advancements in Composite Materials for Aircraft Applications: A Review," *Polymers*, vol. 14, no. 22, 2022.
- [4] R. F. El-Hajjar, D. R. Petersen, "Gaussian function characterization of unnotched tension behavior in a carbon/epoxy composite containing localized fiber

- waviness,” *Composite Structures*, vol. 93, no. 9, pp. 2400–2408, 2011.
- [5] H. M. Hsiao, I. M. Daniel, “Elastic properties of composites with fiber waviness,” *Composites Part A: Applied Science and Manufacturing*, vol. 27, no. 10, pp. 931–941, 1996.
- [6] C. Soutis, J. Lee, “Scaling effects in notched carbon fibre/epoxy composites loaded in compression,” *Journal of Materials Science*, vol. 43, no. 20, pp. 6593–6598, 2008.
- [7] H. Huang, R. Talreja, “Effects of void geometry on elastic properties of unidirectional fiber reinforced composites,” *Composites Science and Technology*, vol. 65, no. 13, pp. 1964–1981, 2005.
- [8] J. Chen, H. Wang, M. Salemi, P. N. Balaguru, “Finite element analysis of composite repair for damaged steel pipeline,” *Coatings*, vol. 11, no. 3, 2021.
- [9] E. Sonat, M. Bakır, S. Özerinç, “Failure behavior of on-site repaired CFRP laminates,” *Composite Structures*, vol. 311, no. June 2022, 2023.
- [10] Hexcel, “Composite Materials and Structures,” 2023. <https://www.hexcel.com/> (accessed Jun. 07, 2023).
- [11] ASTM, “D3039/D3039M Standard Test Method for Tensile Properties of Polymer Matrix Composite Materials.” [https://www.astm.org/d3039\\_d3039m-00.html](https://www.astm.org/d3039_d3039m-00.html) (accessed Jul. 27, 2023).
- [12] H. Bendemra, P. Compston, P. J. Crothers, “Optimisation study of tapered scarf and stepped-lap joints in composite repair patches,” *COMPOSITE STRUCTURE*, vol. 130, pp. 1–8, 2015.
- [13] E. Sonat, “Mechanical Properties of Repaired Carbon Fiber Reinforced Polymer Composites,” Middle East Technical University, 2021.
- [14] S.-H. Ahn, G. S. Springer, “Repair of Composite Laminates-II: Models,” *Journal of Composite Materials*, vol. 32, no. 11, pp. 1076–1114, Jun. 1998. [Online].
- [15] E. Sonat, S. Özerinç, “Failure behavior of scarf-bonded woven fabric CFRP laminates,” *Composite Structures*, vol. 258, no. September 2020, p. 113205, 2021.
- [16] Henkel, “LOCTITE® EA 9396 AERO,” 2023. [https://www.henkel-adhesives.com/vn/en/product/industrial-adhesives/loctite\\_ea\\_9396\\_aero0.html](https://www.henkel-adhesives.com/vn/en/product/industrial-adhesives/loctite_ea_9396_aero0.html) (accessed Jun. 07, 2023).
- [17] T. J, S. W, E. P, Y.-K. Y, “Shear Stress-Strain Data for Structural Adhesives,” 1997.
- [18] Solvay, “FM 300,” 2023. <https://www.solvay.com/en/product/fm-300> (accessed Jun. 07, 2023).
- [19] M. Kashfuddoja, M. Ramji, “Assessment of local strain field in adhesive layer of an unsymmetrically repaired CFRP panel using digital image correlation,” *International Journal of Adhesion and Adhesives*, vol. 57, pp. 57–69, 2015.
- [20] B. D. Agarwal, L. J. Broutman, *Analysis and Performance of Fiber Composites*, 3rd ed. Wiley Blackwell, 1980.
- [21] V. K. S. Choo, *Fundamentals of Composite Materials*. Knowen Academic Press, 1990.
- [22] R. M. Christensen, *Mechanics of Composite Materials*. Dover Publications, 2005.
- [23] I. M. Daniel, O. Ishai, *Engineering Mechanics of Composite Materials*, 2nd ed. Oxford University Press, 2005.
- [24] D. Gay, *Composite Materials: Design and Applications*. CRC Press, 2014.
- [25] Z. Hashin, B. W. Rosen, E. A. Humphreys,

- C. Newton, S. Chatterjee, "Fiber Composite Analysis and Design: Composite Materials and Laminates, Volume 1," 1997.
- [26] L. P. Kollar, G. S. Springer, *Mechanics of Composite Structures*. Cambridge University Press, 2002.
- [27] M. Piggott, *Load Bearing Fibre Composites*. Kluwer Academic Publishers, 2002.
- [28] G. H. Stabb, *Laminar Composites*. Butterworth-Heinemann, 2015.
- [29] S. W. Tsai, H. T. Hahn, *Introduction to Composite Materials*. Technomic Publishing, 1980.
- [30] M. E. Tuttle, *Structural Analysis of Polymeric Composite Materials*. Marcel Dekker Inc., 2004.
- [31] V. V. Vasiliev, E. V. Morozov, *Mechanics and Analysis of Composite Materials*. Elsevier Ltd., 2001.
- [32] J. R. Vinson, R. L. Sierakowski, *The Behavior of Structures Composed of Composite Materials*, 2nd ed. Kluwer Academic Publishers, 2004.
- [33] L. J. Hart-Smith, D. Brown, S. Wong, "Surface Preparations for Ensuring that the Glue Will Stick in Bonded Composite Structures," in *Handbook of Composites*, Boston, MA: Springer US, 1998, pp. 667–685.
- [34] F. C. Campbell, "Secondary Adhesive Bonding of Polymer-Matrix Composites," in *Composites*, ASM International, 2001, pp. 620–632.
- [35] J. P. A. Valente, R. D. S. G. Campilho, E. A. S. Marques, J. J. M. Machado, L. F. M. da Silva, "Adhesive joint analysis under tensile impact loads by cohesive zone modelling," *Composite Structures*, vol. 222, no. January, p. 110894, 2019.